The concentrations of electrolytes in charged cylindrical pores: The hydrostatic hypernetted chain/mean spherical approximation

Parisa Zaini and Hamid Modarress
Department of Chemical Engineering, Amirkabir University of Technology, 424 Hafez Avenue, Tehran, Iran

G. Ali Mansoori[a)]
Department of Chemical Engineering, University of Illinois, 810 S. Clinton Street, Chicago, Illinois 60607-7000

(Received 21 August 1995; accepted 1 December 1995)

The zeroth order (hydrostatic) approximation for inhomogeneous system is applied in the hypernetted chain/mean spherical (HNC/MSA) equations for charged cylindrical pores. The derived equations are introduced as hydrostatic hypernetted chain/mean spherical approximation (HHNC/MSA). These equations are solved using the collocation version of the finite element method. Equilibrium density profiles and mean electrostatic potential profiles are presented and compared with the results of HNC/MSA equations. Density profiles and Exclusion coefficient profiles for 1:1 and 1:2 electrolytes are also compared with the grand canonical Monte Carlo (GCMC) data. Good agreement between the present calculations and GCMC data are observed. Quantitative differences between the present calculations and HNC/MSA are found which are especially significant for large pore diameters and high electrolyte concentrations. © *1996 American Institute of Physics.* [S0021-9606(96)50510-0]

INTRODUCTION

A material containing charged micropores, surrounded by bulk electrolyte, may contain a different concentration of electrolyte than the surrounding solution. The study of this apparently simple phenomenon, the distribution of electrolyte between the porous phase and the bulk solution, is fundamental to many chemical, biological and engineering processes, and recently has become the subject of considerable theoretical and experimental activities.[1]

Materials containing charged micropores, such as ion-exchange resins, cellophane membranes, glass, and certain clays, have long been known to have the property of partially ''*rejecting*'' an electrolyte which is filtered through them.[2–6] Most frequently the electrolyte is dilute and aqueous, and the concentration of the invading electrolyte turns out to be lower in the porous phase than in the surrounding aqueous phase, hence the term ''rejection'' of electrolyte has been used to explain this phenomenon.

The ability of porous materials to exclude an electrolyte forms the basis of important technological processes such as the desalination of water. There are also other phenomena in which the equilibrium distribution of ions plays an essential role, such as electrochemical energy conversion studies,[7,8] and the theory of ion-exchange resins.[9]

The equilibrium structure of electrolytes confined to the pores, will determine the net pressure on the charged surfaces and will influence the flow of electrolyte through the pore.

The classical approach to the study of the ionic concentration is to solve the Poisson–Boltzman (PB) equation. The PB theory fails in some cases and has been substituted by other integral equation theories. For the cylindrical geometry this has an analytical solution only in its linearized form.[10] The PB theory under especial conditions, which include high surface charge density, high electrolyte concentration, or ionic valences greater than one, has large error. This is due to the fact that this approach ignores the size of the ions. In the recent 20 years, many developments have been made for statistical mechanical theories of fluids.[11–14] The hypernetted chain/mean spherical approximation (HNC/MSA) which is also based on statistical mechanics, has been applied for planar,[12] spherical,[13] and cylindrical[14] systems and also for electrolytes confined between two planar electrical double layer's (EDL).[15]

Computer simulation of electrical double layer inside charged cylinders have been made by Jannik and Vlachy for symmetrical and unsymmetrical salts.[16] This simulation which has been made using Monte Carlo (MC) method in a grand canonical ensemble, has been used as a substitution for the experimental measurements.

An earlier HNC/MSA study of the cylindrical pore was carried out by Vlachy and McQuarrie using the planar double-layer version of MSA.[17] Other integral equation approaches to cylindrical pores include the work of Zhou and Stell on uncharged hard-sphere fluids.[18] A more complete form of this equation for cylindrical EDL considering angular dependence of the ion–ion interactions, was derived by Yeomans *et al.*[19] All these equations are based on direct application of the homogeneous Ornstein–Zernike (OZ) equation to inhomogeneous fluids, called the direct method (DM).[20] Although these equations are successful there is still a need for more accurate equation based on a comprehensive model. Many modified equations have been proposed for homogeneous systems but not for inhomogeneous systems. Zhou and Stell,[21] have used the two-body Ornstein–Zernike

[a)]Author to whom correspondence should be addressed.

 0021-9606/96/104(10)/3832/9/$10.00

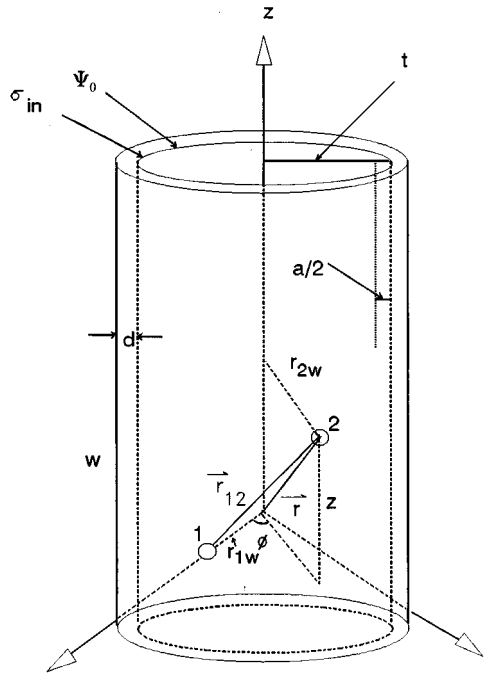

FIG. 1. Geometry for the cylindrical pore.

(OZ) equation along with nonlocal density functional theory for the direct correlation function and have derived new approximations, which are called zeroth order (hydrostatic) approximation. This is called hydrostatic approximation because it becomes exact for inhomogeneities caused by a field varying on a length scale that becomes infinite with respect to the molecular scale, i.e., it exactly describes the hydrostatic of a continuum fluid in a slowly varying field. In this approximation a series of cluster diagrams, named bridge diagrams, which had not been included in HNC approximation have been considered. The HNC approximation will be exact by including the exact bridge function, which is sum of all bridge diagrams,[22] an approximation to the bridge function is the subject of the present paper.

The hydrostatic approach mentioned earlier has been applied here and a new equation is obtained which is introduced as hydrostatic hypernetted chain/mean spherical approximation (HHNC/MSA) for the first time. This equation is solved by the finite element method and the profiles for positive and negative ion distribution function, mean electrostatic potentials of surface and bridge function are obtained as a function of distance from the cylinder surface. Also comparisons with MC calculations are made and good agreements have been observed.

HHNC/MSA MODEL FOR INHOMOGENEOUS SYSTEMS

The cylindrical pore model

As in previous studies,[19] we treat the electrolyte within the restrictive primitive model (RPM). In this model the ions are charged hard spheres of equal diameter (a), with point charges, $Z_+(e)$ and $Z_-(e)$, embedded in their centers. The solvent is considered to be a continuous medium of dielectric constant (ϵ). The pore is an infinitely long hard cylinder (such that edge effects can be ignored) of radius (t) with a uniformly distributed charge density on the inner surface. The pore is composed of a material with the same dielectric constant as the solvent, such that image forces need not be considered. This is the same model employed by earlier workers on this problem.[13,18,20] A diagram of the model system and the geometry used to describe it are found in Fig. 1. Consider the electrolyte with two electrolyte species which are shown as particles 1 and 2, where r_{1w} and r_{2w} are perpendicular distances of particles 1 and 2 to the cylinder axis, respectively.

The HNC/MSA theory and equations

The HNC/MSA theory for a cylindrical pore was previously derived through the direct method (DM),[20] which starts from the homogeneous Ornstein–Zernike (OZ) equation for a multicomponent system of m species. For the charge cylindrical capillary the OZ equation will be

$$h_{wi}(r_{1w}) = c_{wi}(r_{1w}) + \sum_{m}^{2} \rho_m \int h_{wm}(r_{1w}) c_{mi}(r_{12}) dr_w , \tag{1}$$

where (w) represents the wall of the cylinder at infinite dilution and (i) corresponds to ionic species, $g_{wi}(r_{1w}) = h_{wi}(r_{1w}) + 1$ is the radial distribution function between the ionic species and the wall of the cylinder, $c_{mi}(r_{12})$ is the direct correlation function between particles 1 and 2 of the species m and i, and ρ_m is the number density of the species m.

In the HNC/MSA theory the direct correlation function between the cylinder and the ion, $c_{wi}(r_{1w})$, is described by the hyperneted chain approximation (HNC),

$$c_{wi}(r_{1w}) = h_{wi}(r_{1w}) - \ln g_{wi}(r_{1w}) - \beta u_{wi}(r_{1w}), \tag{2}$$

where $u_{wi}(r_{1w})$ is the pair interaction potential between ionic particles (i) and the wall (w), and $\beta = 1/(kT)$. For the ion–ion direct correlation function, $C_{mi}(r_{12})$, the mean spherical approximation (MSA) is employed,

$$r_{12} c_{mi}(r_{12}) = r_{12} c_{\text{sum}}(r_{12}) + Z_m Z_i r_{12} c_{\text{dif}}^{\text{SR}}(r_{12}) - \frac{\beta e^2 Z_m Z_i}{\epsilon} r_{12} > = 0. \tag{3}$$

Expressions for c_{sum}, c_{dif} are given in Appendix A. Substituting the expressions from Eqs. (2) and (3) into Eq. (1) and after some algebraic manipulations, the following equation for inside of the cylinder has been obtained:[19]

$$g_{wi}(r_{1w}) = \exp\Bigg(-e\beta Z_i \psi_0 + \int_0^{t-a/2} K(r_{1w}, r_{2w}) \rho_{ws}(r_{2w}) \times dr_{2w} + A'(r_{1w}) + Z_i \int_0^{t-a/2} L'(r_{1w}, r_{2w}) \times \rho_{wd}(r_{2w}) dr_{2w} \Bigg) \quad 0 \leqslant r_{1w} \leqslant t - a/2, \tag{4}$$

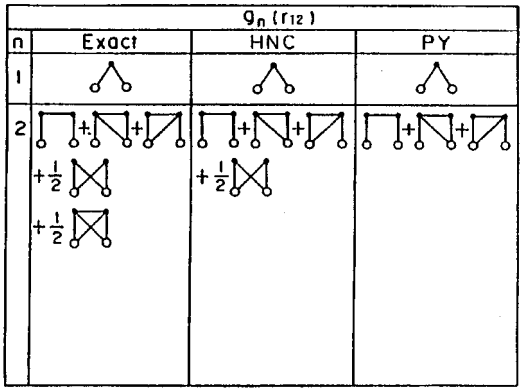

FIG. 2. Exact and approximate (HNC and PY) cluster diagrams involved in the first two terms of the density expansion for the radial distribution function of a homogeneous one component fluid.

where ψ_0 is the constant mean electrostatic potential at the surface and the expressions for ρ_{wd}, ρ_{ws}, $L(r_{1w},r_{2w})$, $K(r_{1w},r_{2w})$, and $A(r_{1w})$ are found in Appendix B.

A shortcoming of Eq. (4) is that a Gauss's law has to be used to derive the interaction potential between ions and the cylinder and the integrals have to be converted to the r_{2w} domain. A similar equation has been derived for the radial distribution function of particles outside of the cylinder,[19] which is not needed in the present calculation. If one takes the point ion limit of Eq. (4) the nonlinear Poisson–Boltzman equation is obtained. This can be seen by setting $A(r_{1w})=K(r_{1w},r_{2w})=L(r_{1w},r_{2w})=0$.

In calculations involving the HNC/MSA equation in the past, electrolytes of the kinds 1:1 and 2:2 at low concentrations were considered for which the bridge functions were not included.[19] Since, according to Zhou and Stell, the hydrostatic HNC(HHNC) which includes this function, is much superior to HNC for fluids near walls,[22] we attempt to modify the HHNC/MSA by applying the hydrostatic approximation.

Inclusion of bridge function

Density expansions of the direct correlation function, the radial distribution function, and the total correlation function can be made. These expansions can be expressed in terms of diagram.[18] In the diagrammatic language, the various approximated integral equations theories correspond to different sets of diagrams. The density expansion for the radial distribution function of a homogeneous one-component fluid is given by[20]

$$g(r_{12})=[1+f(r_{12})]\left[1+\sum_{n=1}^{\text{infinity}}\rho^n g_n(r_{12})\right], \tag{5}$$

where $f(r_{12})=e^{-\beta u(r_{12})}-1$ and $u(r_{12})$ is the interaction potential between particles (1) and (2).

In Fig. 2 the diagrams corresponding to the first two terms in the density expansion are shown. In the HNC approximation one diagram is missing, and in the Percus–Yevick (PY) approximation two diagrams are missing, with respect to the exact expansion. The diagrams missing in the HNC column belong to a class of diagrams called "bridge diagrams." Although the HNC approximation has more diagrams than the PY approximation it is not necessarily better than the PY approximation. Nevertheless, the HNC approximation is better if applied to charged liquids. The bridge diagrams can be reinstated via the inclusion of the bridge function, $B(r)$[22]

$$g(r_{12})=\exp[-\beta u(r_{12})+h(r_{12})-c(\rho,r_{12})+B(r_{12})]. \tag{6}$$

Zhou and Stell have used an exact nonlocal density-functional expansion procedure for direct correlation function for various inhomogeneous systems and they derived nonlocal integral equation approximations, which includes bridge function.

According to their work, when an external force, which causes the inhomogeneity, is identified as the pair potential $u(r)$ between any particle at r and a "source particle" at the origin, (i.e., for a homogeneous system), $B(r)$ equation can be expanded in terms of density

$$B(r)=b_2(r)\rho^2+b_3(r)\rho^3+\cdots, \tag{7}$$

where for the hard sphere system,

$$b_2(r)=15\left(\frac{\pi}{6}\right)^2[h_0^*(r)]^2, \tag{8}$$

$$b_3(r)=\left(\frac{\pi}{6}\right)^3\{30h_0^*(r)h_1^*(r)+24.48[h_0^*(r)]^2\times[3+h_0^*(r)]\} \tag{9}$$

with

$$h_0^*(r)=-(1-r)^3-\frac{r(17r^2-48r+36)}{16} \quad r<1,$$

$$h_0^*(r)=-\frac{(r-2)^2(r+4)}{16} \quad 1<r<2,$$

$$h_0^*(r)=0 \quad r>2, \tag{10}$$

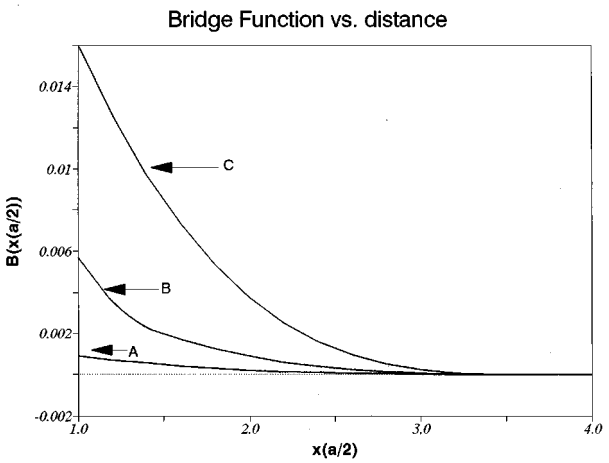

FIG. 3. Bridge function versus distance to the cylinder surface for a model monovalent (1:1) electrolyte at various concentrations of electrolytes (ρ). x is the distance to the inner surface of the cylinder, measured in ionic radii ($a=4.25\times10^{-10}$ m), and $t=4a/2$ (where t is the radius of the cylinder). (A) $\rho=0.5$ M, (B) $\rho=1.0$ M, (C) $\rho=2.0$ M.

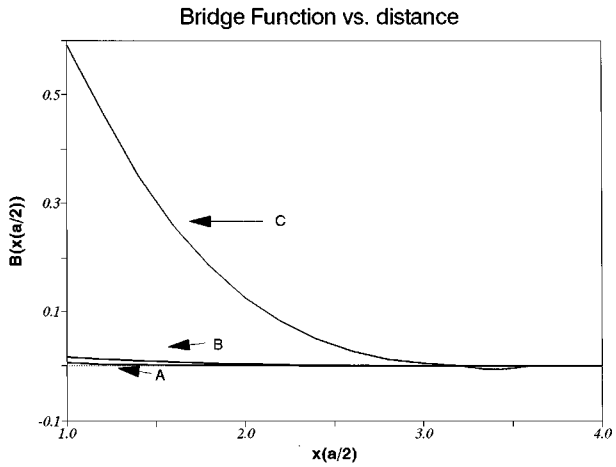

FIG. 4. The same as in Fig. 3 ($t=4a/2$), but at (A) $\rho=1.0$ M, (B) $\rho=2.0$ M, (C) $\rho=10$ M.

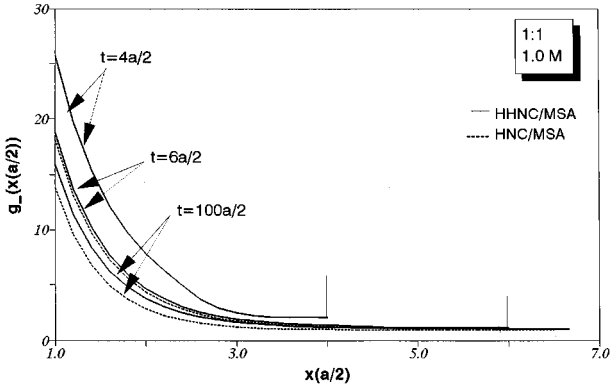

FIG. 5. Counterion distribution functions for a model monovalent electrolyte (1:1); $Z_+=|Z_-|=1$, based on HNC/MSA and HHNC/MSA ($a=4.25\times10^{-10}$ m, $T=298$ K, $\epsilon=78.5$ C^2/N m^2, $\psi_0=105$ mV) confined within a cylindrical pore of radius t where x is the distance to the inner surface of the cylinder. For each cylinder only half the profile is shown since the other half is by symmetry its mirror image.

$$h_1^*(r)=-\frac{-\pi r(r^5-63r^3+70r^2+315r-525)}{1680r} \quad r<1,$$

$$h_1^*(r)=-\frac{\pi(231r^2-595r+162)}{1680r} \quad 1<r<2,$$

$$h_1^*(r)=\frac{\pi(r-3)^4(r^3+12r^2+27r-6)}{1680r} \quad r>2,$$

$$h_1^*(r)=0 \quad r>3, \tag{11}$$

where the hard sphere diameter has been taken as 1.

We know that the bridge function dose not depend strongly on the intermolecular potential. Therefore, if $B(r)$ can be parametrized accurately for some fluids, such as the hard sphere fluid, the resulting $B(r)$ can be used in many other applications.[22]

From this fact and since with the DM one can convert a two component inhomogeneous system to a three component homogeneous system, we have used $B(r)$ equation of homogeneous hard sphere system to our system which like previous studies have considered as a three component homogeneous system (cylinder cause inhomogeneity).

Then we have the following equation (HHNC equation) for direct correlation function between an ion and the cylinder:

$$c_{wi}(r_{1w})=h_{wi}(r_{1w})-\ln g_{wi}(r_{1w})-\beta u_{wi}(r_{1w}) - B_{wi}(r_{1w}), \tag{12}$$

where r_{1w} is the distance of ion from cylinder axis.

Since r in the expressions for $B(r)$ is the distance from surface of cylinder (cylinder is the particle at origin), we must use the following conversion in the expressions:

$$r=\frac{t-r_{1w}}{t}. \tag{13}$$

Then we have the HHNC/MSA equation for inside of the cylinder

$$g_{wi}(r_{1w})=\exp\left(-e\beta Z_i\psi_0+\int_0^{t-a/2}K(r_{1w},r_{2w})\rho_{ws}(r_{2w}) \times dr_{2w}+A'(r_{1w})+Z_i\int_0^{t-a/2}L'(r_{1w},r_{2w}) \times\rho_{wd}(r_{2w})dr_{2w}-B_{wi}(r_{1w})\right) \quad 0\leq r_{1w}\leq t-a/2, \tag{14}$$

where

$$B_{wi}(r_{1w})=b_2(r_{1w})\rho_i^2+b_3(r_{1w})\rho_i^3, \tag{15}$$

$$\rho_i=\rho_m a^3. \tag{16}$$

Method of calculation

We have solved the HHNC/MSA equation using collocation version of the finite element method.[23] The goal of the finite element method is to reduce a set of equations to a system of linear algebraic equations by subdividing the domain of the problem into a number of subdomains, or elements, of appropriate size and shape. The solution functions, $h_i(x)$ are approximated by a set of N linearly independent basis functions $[\varphi_i(x)]$

$$h_i(x)=\sum_{k=1}^{N}h_{ik}\varphi_k(x). \tag{17}$$

The functions $\varphi_k(x)$ have simple mathematical forms and are defined piecewise over the finite element mesh. In this work we have used linear Lagrange basis functions. The unknown expansion coefficients, $\{h_{ik}\}$, are approximations for the values of the solution function $h_i(x)$ evaluated at the nodes of the elements.

In the collocation version of the finite element method the residuals are reduced to zero at the nodes of the elements,

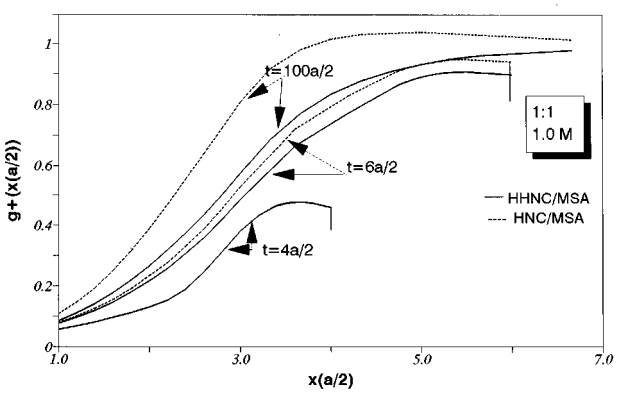

FIG. 6. Coion distribution function for various cylinder diameters. The notations are the same as in Fig. 5 as are the meanings of the curves.

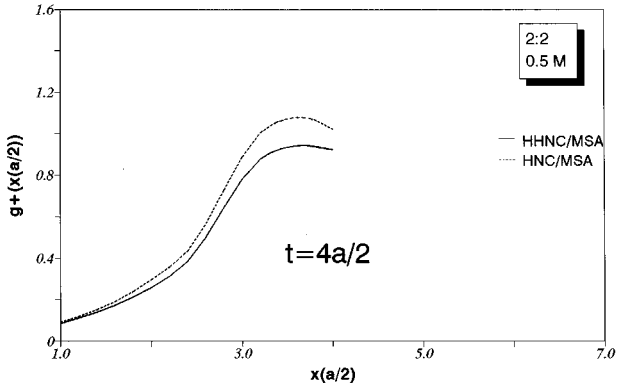

FIG. 8. Coion distribution functions ($t=4a/2$). The notations are the same as in Fig. 6.

$$\int_0^{t-a/2} \mathrm{Re}(h(x)\,\delta(x-x_l)\,dx=0 \tag{18}$$

for $l=1,\ldots,N$, where $\delta(x-x_l)$ is Dirac delta function and x_l is the value of x at the lth node.

Once a set of basis function is selected, equations can be solved by Newton's method. Gaussian elimination is used to solve the set of equations. The iterative process is continued until the Euclidean norm of the difference between successive iterations become less than a prescribed small number Δ

$$\|h^{(k+1)}-h^{(k)}\|=\left[\sum_{i=1}^{n}\sum_{j=1}^{N}(h_{ij}^{(k+1)}-h_{ij}^{(k)})^2\right]^{1/2}\leqslant\Delta, \tag{19}$$

where k is number of iterations and here $\Delta=10^{-9}$.

In what follows the results of calculations considering bridge function in the HHNC/MSA equations are introduced and they are compared with the case when no bridge function are considered (HNC/MSA).

RESULTS AND DISCUSSION

The results of solving Eq. (4) known as HNC/MSA and Eq. (14) named HHNC/MSA by the collocation version of the finite element method are presented here. We have also solved PB equation in order to derive initial guesses for calculations, the results of which are not reported.

All calculations were done with $\epsilon=78.5$ ($C^2/N\,m^2$), $T=298$ K, $a=4.25\times10^{-10}$ m (except for the sake of comparison with the MC results that the calculations were carried out with $a=4.2\times10^{-10}$ m).

Also some results for the bridge function and mean electrostatic potential are presented.

The bridge function profiles of a 1:1 electrolyte and a pore radius $t=4a/2$ are shown in Figs. 3 and 4 as a function of distance to the cylinder surface at various concentrations of electrolytes. It is seen that the bridge function decreases with increasing of the distance and increases with increasing the concentration of the electrolyte.

The radial distribution function profiles calculated based on HNC/MSA and HHNC/MSA are given by Figs. 5–12 at various surface potentials, cylinder radius and various concentrations of electrolytes, as a function of distance to the cylinder surface.

In Figs. 5 and 6 we present results for the density profiles of a 1:1 electrolyte, with 1.0 M concentration and surface potential of 105 mV, at various cylinder diameter ($t=4a/2$, $6a/2$, $100a/2$, where t is the cylinder radius). It is shown that the HHNC/MSA counter ion density profiles stand above the HNC/MSA results and the coion profiles

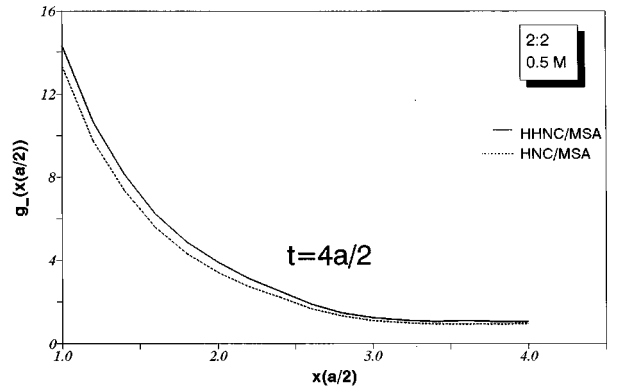

FIG. 7. Counterion distribution functions for a model divalent electrolyte ($a=4.25\times10^{-10}$ m, $\rho=0.5$ M, $Z_+=|Z_-|=2$, $T=298$ K, $\epsilon=78.5$ $C^2/N\,m^2$, $\psi_0=50$ mV).

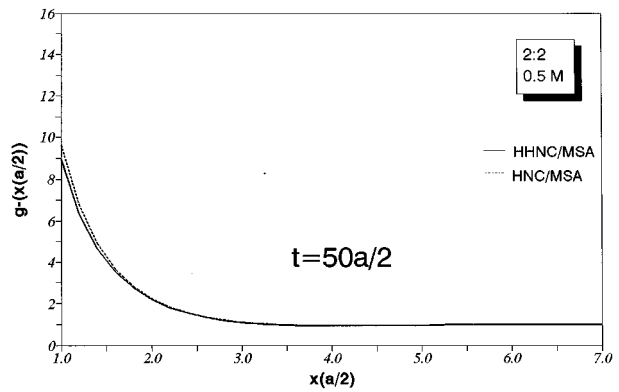

FIG. 9. The same as in Fig. 7 but for $t=50a/2$.

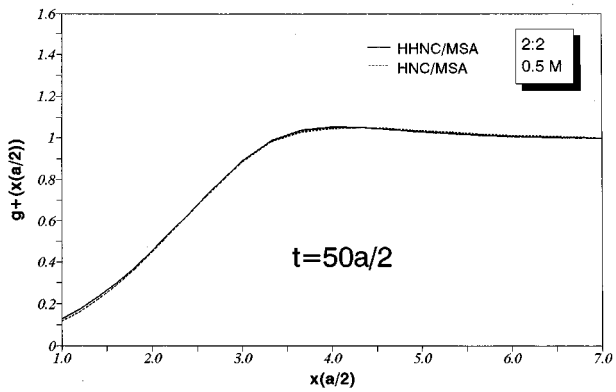

FIG. 10. The same as in Fig. 8 but for $t=50a/2$.

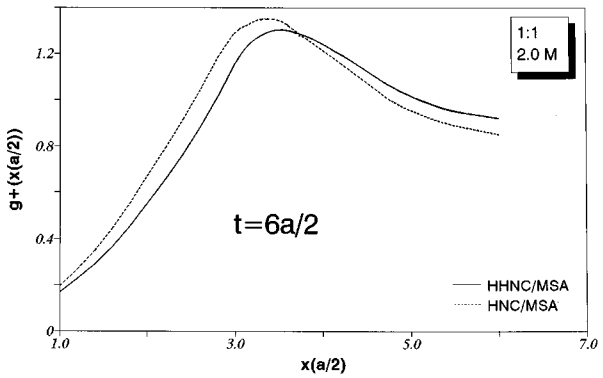

FIG. 12. Coion distribution function for a model monovalent electrolyte, $\rho=2.0$ M.

stand below the HNC/MSA results. We can see that the counterions at surface will be much more strongly held to a charge cylinder in HHNC/MSA than HNC/MSA. That is due to considering bridge function which affects the interactions. This observation suports the idea that the exclusion coefficient which is discussed below should increase by including bridge function.

The exclusion coefficient,[16] which is a convenient measure of electrolyte exclusion from porous phase, is defined as

$$\Gamma \equiv \frac{c_{\text{coion}} - \langle c_{\text{coion}} \rangle}{c_{\text{coion}}},$$

where c_{coion} is the concentration of coions in the bulk electrolyte and $\langle c_{\text{coion}} \rangle$ is the average concentration of coions in the pore.

Also we can see that the difference between the two model increase, with increasing diameter of the cylinder, while the trends of the curves remain the same in both models.

Similar results are shown for a 2:2 electrolyte (0.5 M and 50 mV) in Figs. 7–10. In this case the difference between the two models is less than 1.0 M case. The reason for this effect is probably due to the fact that the bridge function depends highly on the concentration of the electrolyte so that increasing, or decreasing, the electrolyte concentration, directly affects the $B(r)$ and so the profiles.

Density profiles for a 2.0 M, 1:1 electrolyte ($t=6a/2$, $\psi_0=105$ mV) are given in Figs. 11 and 12. which show larger difference than the 1.0 M case due to higher concentration.

In Figs. 13 and 14 the profiles for mean electrostatic potentials are shown as a function of distance. The values calculated by HHNC/MSA case are greater than the HNC/MSA values. The anomalous behavior for $t=3a/2$ is due to the small pore diameter that is probably related to the difficulty in accomodating hard spheres in such a narrow pore.

The mean electrostatic values for two models have also larger difference at high concentrations (see Fig. 15 for $p=2.0$ M).

In Fig. 16 we compare the results of HHNC/MSA for a 1:1 electrolyte and Monte Carlo (MC) data.[16] Since the MC simulation was done at a constant surface charge density (σ) on the inner surface, but leaving surface charge density on the outside free to adjust to the inside condition, the calculations are equivalent to the constant potential case. Thus we have solved the constant potential HHNC/MSA, HNC/MSA and PB equations for various surface potentials until the resulting surface charge density coincide with the MC results. There are good agreements between the HHNC/MSA and MC simulation. The same observation can be made in Fig. 17 for a 1:2 electrolyte.

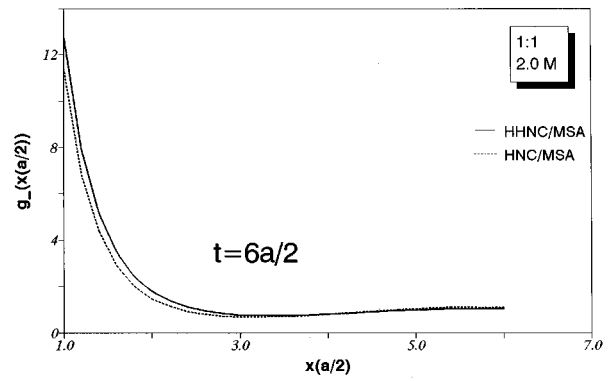

FIG. 11. Counterion distribution function for a model monovalent electrolyte, with $\rho=2.0$ M.

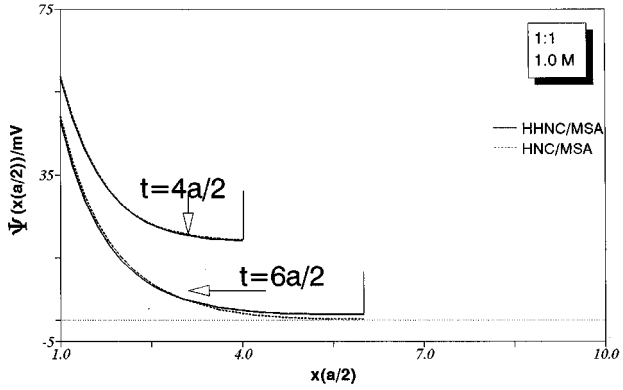

FIG. 13. The mean electrostatic potential as a function of the distance to the inner surface of the cylinder for various cylinder diameters. The parameters are the same as in Fig. 5 as are the meanings of the curves.

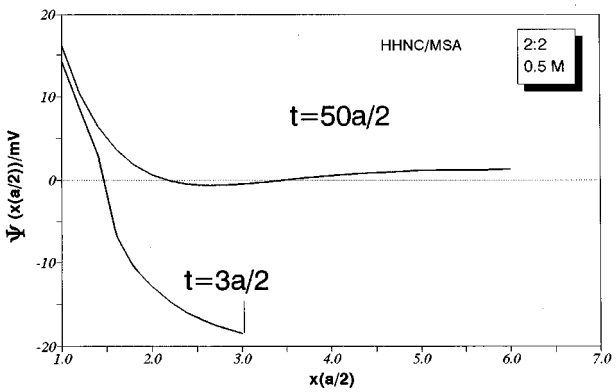

FIG. 14. The mean electrostatic potential as a function of the distance to the inner surface of the cylinder for various cylinder diameters. The parameters are the same as in Fig. 7 as are the meanings of the curves.

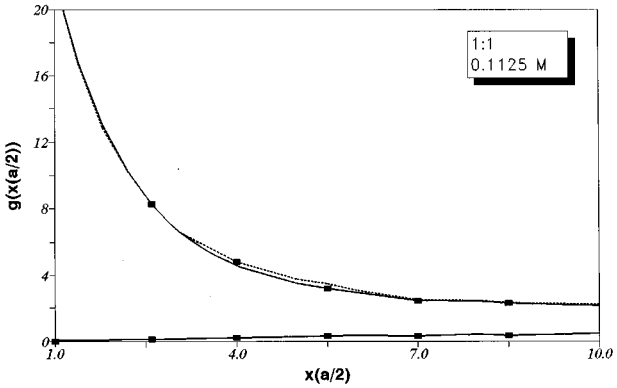

FIG. 16. The counterion and coion distribution functions for a model monovalent electrolyte. The solid curves are the HHNC/MSA results, the dashed curves are the PB results, and the points are the MC results. The radius of the pore is 22.125×10^{-10} m and the surface charge density on the inner surface, σ_{in}, is 0.0712 C/m^2.

One of the important parameters in the study of the electrolytes confined to the pores, is the exclusion coefficient, Γ, where it is compared here for a 1:2 electrolyte, at various surface charge density with the MC data.[16] We can see that the HHNC/MSA values give better results than the PB equation[16] as shown in Fig. 18. It should be noted that since the concentration of the electrolytes in the simulation data for the state shown in Fig. 18 is small, the bridge function is approximately zero. Therefore, the HHNC/MSA and HNC/MSA results coincided with each other.

CONCLUSION

The study of the structure of the electrolytes within a cylinderical pore is an important subject of investigation, but it is at its infancy. In a preliminary study[19] the HNC/MSA equation was used to model this phenomena. In the present report we have demonstrated the importance of considering the bridge function in the study of the ionic concentrations in pores.

The bridge function does not depend strongly on the intermolecular potential. This fact was the basic assumption in our work. In contrast to the potential, the bridge function hardly depends on the concentration of the electrolyte and also on the distance to the cylinder surface (or axis). So it seems to be necessary to consider the bridge function for high electrolyte concentrations and large pore diameters. However, our results indicate that introduction of bridge function significantly alters the concentration profile prediction of ions in pores at higher pore diameters.

The study of the structure of electrolyte within charged cylindrical pores is a challenging theoretical problem of significant practical interest. This technique can be extended to the application of pressure or electrical potential gradients across charged capillaries, in equilibrium with a reservoir containing an electrolyte solution, which can be applied to interesting electrokinetic phenomena such as electro-osmosis, streaming potential and other similar phenomena. Under certain assumptions, the equilibrium density profiles such as the ones reported in this paper can be used to calcu-

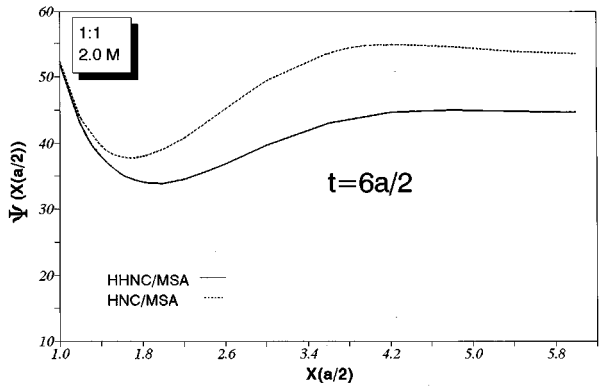

FIG. 15. The same as in Fig. 14 but for $\rho=2.0$ M and $t=6a/2$.

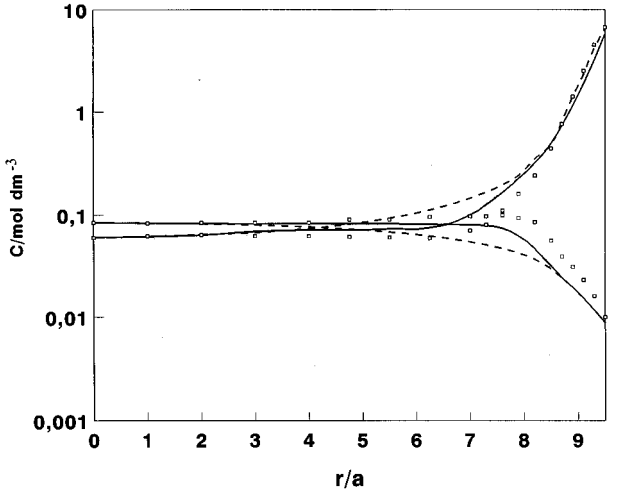

FIG. 17. Concentration profiles for a 1:2 electrolyte ($2Z_+=|Z_-|=2$) with $\rho=0.0475$ M. The solid curves are the HHNC/MSA results, the dashed curves are the PB results and the points are the MC results. The radius of the pore is 22.125×10^{-10} and $\sigma_{in}=0.1425$ C/m^2.

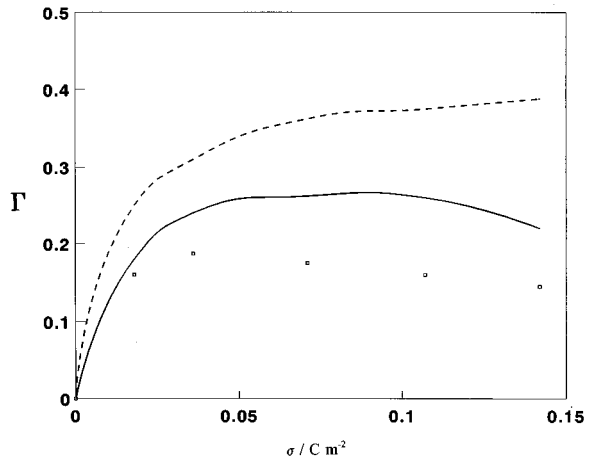

FIG. 18. The exclusion coefficient as a function of the surface charge density for a 1:2 electrolyte with $\rho=0.0476$ M. The solid curve is the HHNC/MSA result, the dashed curve is the PB result and the points are the MC results.

late the net volume flux of solution and the net electrical current.

ACKNOWLEDGMENTS

The authors would like to thank Dr. S. M. Alaei for his help. This research is supported in part (P.Z. and H.M.) by the AKU and in part (GAM) by the National Science Foundation Grant No. CTS-9108595.

APPENDIX A

The expressions for $c_{\rm sum}(r_{12})$ and $c_{\rm dif}^{\rm SR}(r_{12})$ appearing in Eq. (3) are defined by[19]

$$r_{12}c_{\rm sum}(r_{12})=-c_1r_{12}-6\eta c_2r_{12}^2-1/2\,\eta c_3r_{12}^4 \quad r_{12}\leqslant a, \tag{A1}$$

$$r_{12}c_a^{\rm SR}=\frac{e^2\beta}{\epsilon}\left(1-\frac{2\Gamma}{(1+\Gamma a)^2}\,r_{12}+\frac{\Gamma^2}{(1+\Gamma a)^2}\,r_{12}^2\right) \quad r_{12}\leqslant a, \tag{A2}$$

and $c_{\rm sum}(r_{12})=c_{\rm dif}^{\rm SR}(r_{12})=0$ for $r_{12}>a$, where

$$\eta=\frac{1}{6}\,\pi a^3\sum_{m=1}^{n}\rho_m, \tag{A3}$$

$$c_1=\frac{(1+2\eta)^2}{(1-\eta)^4}, \tag{A4}$$

$$c_2=-\frac{(1+0.5\eta)^2}{a(1-\eta)^4}, \tag{A5}$$

$$c_3=\frac{c_1}{a^3}, \tag{A6}$$

$$\Gamma a=-\frac{1}{2}+\frac{1}{2}\sqrt{1+2Ka}, \tag{A7}$$

$$K^2=\frac{4\pi\beta e^2}{\epsilon}\sum_{m=1}^{n}\rho_mZ_m^2. \tag{A8}$$

APPENDIX B

The expressions for ρ_{wd}, ρ_{ws}, $L(r_{1w},r_{2w})$, $K(r_{1w},r_{2w})$ and $A'(r_{1w})$ appearing in Eq. (4) are defined by[19]

$$\rho_{ws}(r_{2w})=\sum_{m=1}^{n}\rho_mh_{wm}(r_{2w}), \tag{B1}$$

$$\rho_{wd}(r_{2w})=\sum_{m=1}^{n}\rho_mZ_mh_{wm}(r_{2w}), \tag{B2}$$

$$L'(r_{1w},r_{2w})=\begin{cases} f'(r_{1w},r_{2w}) & r_{2w}<r_{1w}-a \\ L(r_{1w},r_{2w})+f'(r_{1w},r_{2w}) & r_{1w}-a\leqslant r_{2w}\leqslant r_{1w}+a \\ f'(r_{1w},r_{2w}) & r_{2w}>r_{1w}+a \end{cases} \tag{B3}$$

$$f'(r_{1w},r_{2w})=\frac{2\pi\beta e^2}{\epsilon}\,r_{1w}\,\ln\left(\frac{r_{1w}^2+r_{2w}^2+|r_{1w}^2-r_{2w}^2|}{2t^2}\right), \tag{B4}$$

$$K(r_{1w},r_{2w})=\begin{cases} 0 & r_{2w}<r_{1w}-a \\ -4r_{1w}\displaystyle\int_0^{\varphi_0}(c_1J_0+6\eta c_2J_1+1/2\,\eta c_3J_3)\,d\varphi & r_{1w}-a\leqslant r_{2w}\leqslant r_{1w}+a \\ 0 & r_{2w}>r_{1w}+a \end{cases} \tag{B5}$$

$$L(r_{1w},r_{2w})=\begin{cases} 0 & r_{2w}<r_{1w}-a \\ 4r_{2w}\,\dfrac{e^2\beta}{\epsilon}\displaystyle\int_0^{\varphi_0}\left(J_2-\frac{2\Gamma}{1+\Gamma a}\,J_0+\frac{\Gamma^2}{(1+\Gamma a)^2}\,J_1\right)d\varphi & r_{1w}-a\leqslant r_{2w}\leqslant r_{1w}+a \\ 0 & r_{2w}>r_{1w}+a \end{cases} \tag{B6}$$

where

$$\varphi_0 = \cos^{-1}\left(\frac{r_{1w}^2 + r_{2w}^2 - a^2}{2 r_{1w} r_{2w}}\right), \tag{B7}$$

$$J_0 = \int_0^{z_0} dz, \tag{B8}$$

$$J_1 = \int_0^{z_0} r_{12}\, dz, \tag{B9}$$

$$J_2 = \int_0^{z_0} \frac{1}{r_{12}}\, dz, \tag{B10}$$

$$J_3 = \int_0^{z_0} r_{12}^3\, dz. \tag{B11}$$

These integrals over dz can be done analytically

$$Z_0 = (a^2 - r_{1w}^2 - r_{2w}^2 + 2 r_{1w} r_{2w} \cos\varphi)^{1/2}, \tag{B12}$$

$$A'(r_{1w}) = -\rho \int_{t-a/2}^{r_{1w}+a} dr_{2w}\, K(r_{1w}, r_{2w}). \tag{B13}$$

[1] V. Vlachy and A. D. J. Haymet, Austr. J. Chem. **43**, 1961 (1990); J. Am. Chem. Soc. **111**, 477 (1989).
[2] R. M. Wheaton and W. C. Bauman, Ind. Eng. Chem. **45**, 228 (1953).
[3] A. S. Michaels and C. S. Lin, Ind. Eng. Chem. **47**, 1249 (1955).
[4] F. A. Kraus, A. E. Marcinkowsky, J. S. Johnson, and A. J. Shor, Science **151**, 194 (1966).
[5] A. E. Marcinkowsky, K. A. Kraus, H. O. Philips, J. S. Johnson, Jr., and A. J. Shor, J. Am. Chem. Soc. **88**, 5744 (1966).
[6] J. G. McKelevy, K. S. Spiegler, and M. R. J. Willie, Chem. Eng. Prog., Symp. Ser. **55**, 199 (1959).
[7] M. Tasaka, N. Aoki, Y. Kondo, and M. Nagasawa, J. Phys. Chem. **13**, 1307 (1957).
[8] L. Dresner, J. Phys. Chem. **67**, 1635 (1963).
[9] D. Dolar and V. Vlachy, Vestn. Slov. Kem. Drus. **28**, 327 (1981).
[10] F. Booth, J. Chem. Phys. **19**, 821 (1951).
[11] J. Haile and G. A. Mansoori, *Molecular Based Study of Fluids* (ACS, Washington, D.C., 1981).
[12] M. Lozada-Cassou, R. Saavedra-Barrera, and D. Henderson, J. Chem. Phys. **77**, 5150 (182).
[13] E. Gonzales-Tovar and M. Lozada-Cassou, J. Phys. Chem. **93**, 3761 (1989).
[14] E. Gonzales-Tovar, M. Lozada-Cassou, and D. Henderson, J. Chem. Phys. **83**, 361 (1985).
[15] M. Lozada-Cassou and E. Diaz-Herrera, J. Chem. Phys. **92**, 1194 (1990); *ibid*. **93**, 1386 (1990).
[16] B. Jannik and V. Vlachy, J. Am. Chem. Soc. **115**, 660 (1993).
[17] V. Vlachy and D. A. McQuarrie, J. Phys. Chem. **90**, 3248 (1986).
[18] Y. Zhou and G. Stell, Mol. Phys. **66**, 791 (1989).
[19] L. Yeomans, S. E. Feller, E. Sanchez, and M. Lozada-Cassou, J. Chem. Phys. **98**, 1436 (1993).
[20] D. Henderson, F. F. Abraham, and J. A. Barker, Mol. Phys. **31**, 1291 (1976); M. Lozada-Cassou, in *Fundamentals of Inhomogeneous Fluids*, edited by D. Henderson (Marcel Decker, New York, 1992), Chap. 8.
[21] Y. Zhou and G. Stell, J. Chem. Phys. **92**, 5533 (1990).
[22] R. Evans, in *Fundamentals of Inhomogeneous Fluids*, edited by D. Henderson (Marcel Decker, New York, 1992), Chap. 3.
[23] J. N. Reddy, *An Introduction to the Finite Element Method* (McGraw-Hill, New York, 1985).